Journal of Thermal Science and Technology

Vol. 5, No. 2, 2010

Evaluation of the Flame Lift-off Length in Diesel Spray Combustion Based on Flame Extinction*

Ulugbek AZIMOV**, Nobuyuki KAWAHARA**, Eiji TOMITA** and Kazuya TSUBOI**

**Department of Mechanical Engineering, Okayama University, Tsushima –Naka 3, Okayama, 700-8530, Japan

E-mail: uazimov2001@yahoo.com

Abstract

The interaction of spray and combustion processes forms a complex system of physical phenomena undergoing in IC engines. Studying this interaction is important to determine strategies for simultaneously reducing soot and NOx emissions from diesel engines. Spray combustion interactions are evaluated by the flame lift-off length - the distance from the injector orifice to the location of hydroxyl luminescence closest to the injector in the flame jet. Various works have been dedicated to successful simulations of lifted flames of a diesel jet by use of various combustion modeling approaches. In this work, flame surface density and flamelet concepts were used to model the diesel lift-off length. Numerical studies have been performed with the ECFM3Z model and n-Heptane fuel to determine the flame lift-off length under quiescent conditions. The numerical results showed good agreement with experimental data, which were obtained from an optically accessible constant volume chamber and presented at the Engine Combustion Network (ECN) of Sandia National Laboratories. It was shown that at a certain distance downstream from the injector orifice, stoichiometric scalar dissipation rate matched the extinction scalar dissipation rate. This computed extinction scalar dissipation rate correlated well with the flame lift-off length. For the range of conditions investigated, adequate quantitative agreement was obtained with the experimental measurements of lift-off length under various ambient gas O_2 concentrations and ambient gas densities.

Key words: Spray Combustion, Lift-off Length, ECFM3Z Model, Scalar Dissipation

1. Introduction

The interaction of spray and combustion processes forms a complex system of physical phenomena whose time and length scales range over a wide spectrum. This interaction plays an important role in engine performance and exhaust emissions. The new combustion strategies focused on simultaneous reduction of NOx and soot emissions suggest that ignition timing is controlled to be delayed after the end of injection. Therefore, air in the combustion chamber can be properly utilized by optimizing the air-fuel mixing in the spray. To describe air-fuel mixing, the diesel flame lift-off length is evaluated. The lift-off length, as an indicator of local mixture formation, is the driving parameter for identifying the combustion rate and pollutant formation. Peters [1] conducted an extensive research on lift-off length. At the macroscopic level, this research indicates that the flame stabilization occurs along the stoichiometric mixture contour, at a location where a balance exist between

*Received 10 June, 2010 (No. 10-0247)
[DOI: 10.1299/jtst.5.238]

the convective flow downstream in the jet and turbulent flame propagation upstream. The flame stabilization process is controlled by a complex set of interactions between turbulent fluid mechanics and flame chemistry processes [2-5]. Recent experimental results proved the fact that after the initial autoignition phase, the reaction zone of a diesel fuel jet stabilizes at a location downstream of the fuel injector [6]. The flame remains lifted during the diffusion-burn phase of heat release, allowing fuel and ambient gases to premix upstream of the reaction zone and strongly affecting combustion and soot formation processes downstream [7, 8]. The oxygen in the entrained air is believed to react with fuel in a rich reaction zone in the central region of the spray just downstream of the lift-off length [9, 10]. The products of such a rich reaction zone are ideal for forming soot, suggesting a strong link between soot formation and the amount of air entrainment, or fuel-air mixing, that occurs upstream of the location of flame lift-off. More air-entrainment upstream of the lift-off length is likely to lead to less soot formation.

Lift-off length was modeled and simulated by several researchers. Senecal *et al.* [11] performed a multi-dimensional modeling of the direct-injection diesel flame lift-off length using CFD and parallel detailed chemistry. They applied KIVA/SAGE modeling methodology to model experiments of Siebers and Higgins [7]. Tap and Veynante [12] simulated the flame lift-off length of a diesel jet by using the generalized surface density modeling approach. This modeling approach was coupled to a mixing model and a chemistry model, based on the unsteady flamelet equations in the flamelet library. Lehtiniemi *et al*. [13] modeled the lift-off length using detailed chemistry and the progress variable approach. Venugopal and Abraham [14, 15] modeled the lift-off length and correlated it with flame extinction. For the range of conditions explored, adequate agreement was obtained between the numerical results and the measurements for varying injection pressures, ambient densities, ambient temperatures and ambient O_2 concentrations. D'Errico *et al.* [16] compared the lift-off length computed with the Eddy Dissipation Model (EDM) and Partially Stirred Reactor Model (PaSR). Singh *et al.* [17] validated hybrid auto-ignition/flame-propagation model against flame lift-off. Campbell *et al*. [18] performed the analysis of premixed flame and lift-off length in diesel spray combustion with multi-dimensional CFD. Vishvanathan and Reitz [19] predicted the diesel flame lift-off length under low-temperature combustion conditions. Karrholm *et al.* [20] performed 3-D simulations of the diesel lift-off length using OpenFoam and KIVA-3V CFD codes with n-Heptane reaction mechanism involving 83 species and 338 reactions.

Flame lift-off is challenging to model because of its complex nature in association with turbulence and chemistry that result in local quenching, partial-premixing and flame propagation. The previous research mentioned above could not recommend a single threshold temperature value that might be applied to the wide range of diesel combustion conditions, including the combustion at diluted ambient gas with smaller Damkohler number, as observed in LTC. The merit of the approach proposed in this paper is that it takes into account turbulence and chemistry interactions, autoignition and flame propagation and that the lift-off length is evaluated using the ECFM3Z model based on the flame surface density and flame extinction concept. Because it is confirmed that the lift-off length is strongly affected by turbulence and chemistry interactions, autoignition and flame propagation [1, 6, 9]. This is the original study that uses ECFM3Z model to evaluate the lift-off length based on flame extinction.

The modeling results were compared with available experimental data from the Engine Combustion Network of Sandia National Laboratories [21]. n-Heptane was used as the surrogate diesel fuel, and the flamelet library was generated based on the values of pressure, temperature, O_2 concentration, reaction progress rate and scalar dissipation rate. The influences of the chamber density and ambient gas O_2 concentration on the lift-off length were investigated.

2. Description of ECFM3Z model

The reliability of any combustion model depends on its accuracy of predicting the mixing between fuel and oxidizer or between the fresh and the burned gases. ECFM3Z model tries to address the mixing problem in a convenient way for engine combustion simulations. In ECFM3Z combustion model, combustion is described in terms of a progress variable $(\widetilde{c})$ and a mixture fraction $(\widetilde{Z})$. A diagram of the ECFM3Z model structure is presented in Figure 1. According to this representation, each computational cell is divided into three subgrid regions in the mixture fraction *Z* space: the unmixed fuel region, the mixing region containing fuel, air and residual gases, and the unmixed air+residual gases region. This structure can be seen as a simplified CMC approach where the *Z* space contains only three points. In the original ECFM3Z model [22], this structure was represented with the presumption of the probability density function (pdf) of the mixture fraction variable *Z* as three different Dirac distributions:

$$P(Z) = \underbrace{\alpha\delta(Z)}_{\substack{Unmixed\ \ Air+EGR\ \ Region}} + \underbrace{\beta\delta(1-Z)}_{Unmixed\ \ Fuel\ \ Region} + \underbrace{\gamma\delta(Z-\overline{Z})}_{Mixed\ \ Region} \tag{1}$$

where α, β, γ are the coefficients that determine the weighting factor of each region. $\overline{Z}$ is the average value of the mixture fraction in the mixed region. The first Dirac function corresponds to the unmixed air+EGR region, the second one to the unmixed fuel region and the third one to the mixed region. Here, the mixture fraction is defined as the fuel tracer species Y_{TF}, which corresponds to the fuel mass fraction before the onset of combustion. Reactions cannot take place in the unmixed fuel region and the unmixed air+EGR region; they are only possible inside the mixing region. Combustion calculations are thus conducted for this region according to the description in [22]. The subgrid cell mixing region is in turn divided into zones of unburned and burned gases.

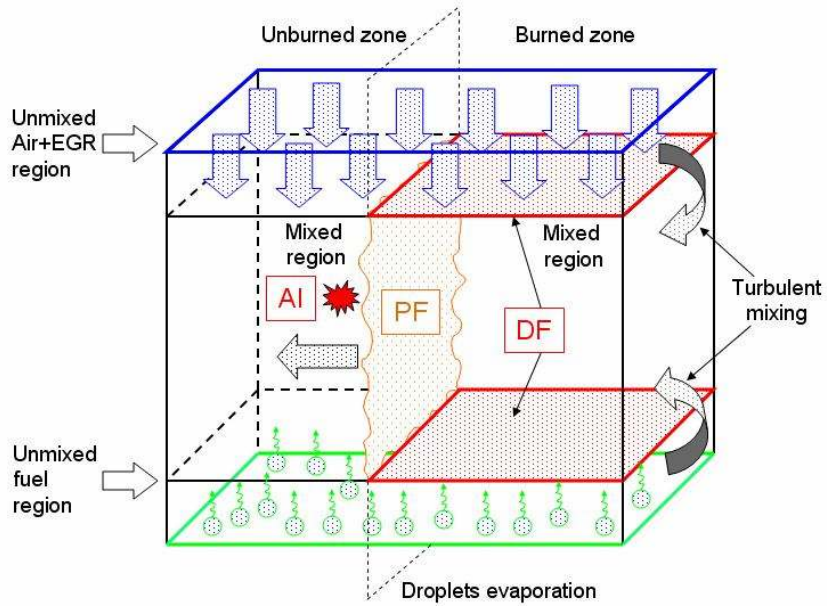

Figure 1. Schematics of ECFM3Z model

3. Flame lift-off length modeling

Different modeling approaches were addressed to compute the diesel lift-off length [11-20], as was mentioned earlier. In this paper, the lift-off length is modeled based on flame surface density and the flame extinction concept.

To compute the diesel jet lift–off length, the mean scalar dissipation rate at stoichiometric conditions, χ_{st}, is determined.

$$\tilde{\chi}_{st} = C_{\chi} \frac{\tilde{\varepsilon}}{\tilde{k}} \tilde{Z}^{"2} \tag{2}$$

where ε and k are the Reynolds-averaged turbulent dissipation rate and the turbulent kinetic energy. $\tilde{Z}^{"2}$ is the variance of mixture fraction Z. The scalar time scale ratio C_{χ} is assumed to be a constant [1]. One-dimensional laminar flamelet equations are used to compute the structure of a laminar diffusion flame for the range of conditions in this paper.

$$\rho \frac{\partial Y_i}{\partial t} = \rho \frac{\chi}{2} \frac{\partial^2 Y_i}{\partial Z^2} + \dot{\omega} \tag{3}$$

$$\rho \frac{\partial T}{\partial t} = \rho \frac{\chi}{2} \frac{\partial^2 T}{\partial Z^2} + \frac{1}{c_p} \frac{\partial p}{\partial t} - \sum_{i=1}^{n} \frac{h_i^0}{c_p} \dot{\omega}_i \tag{4}$$

where p-gas pressure, T-temperature, ρ-mixture mass density, Y_i- mass fraction, $\dot{\omega}$-production/destruction rate, and h_i – specific enthalpy of species i, c_p - mixture specific heat. All the species are assumed to have the same mass diffusion coefficient equal to the thermal diffusivity of the mixture.

The scalar dissipation rate represents the extent of heat conduction and species diffusion at the flame. The flame structure consists essentially of a thin inner reaction zone embedded between two chemically inert outer zones. When χ_{st} is increased, heat conduction from and reactant diffusion to the reaction zone will increase. If this increase is beyond a critical value, χ_{ext}, incomplete reaction results in reactant leakage, and thus heat conduction can no longer be balanced by heat production due to chemical reaction, and the flame is extinguished. This behavior is described by the well-known S-shaped curve [1]. Extinction occurs when the characteristic time of flow of reactants through the reaction zone becomes shorter than the time required for heat release through chemical reaction, or as the Damkohler number, Da, that is inversely proportional to χ_{st}, is reduced to a critical value.

4. Simulation procedure

To accurately evaluate spray and combustion processes at different conditions, it is critical that the dependence of these processes on grid size is minimized. In this work, prior to the modeling of the lift-off length, grids with cell sizes of 0.25mm, 0.5mm, 1mm and 2mm were evaluated for vaporizing spray distributions and these distributions were compared with ones from experiment. The dependence of flow parameters on grid size was investigated for the conditions at fuel injection pressure, P_{inj}=135 MPa; nozzle orifice diameter, $D_{orifice}$=0.163 mm; discharge coefficient, C_D=0.86; nozzle length-to-diameter ratio, L/D-5.52; spray angle θ/2=9°; ambient gas pressure P_{amb}=4 MPa; and ambient gas

temperature T_{amb}=820 K. The 3-D computational grid, a cylinder-shaped constant volume chamber 80mm in diameter and 80 mm in length, was discretized with hexahedral cells of 2mm, 1mm, 0.5mm and 0.25mm in size. Fuel vapor penetration was also compared at the conditions with the shadowgraph experimental results available at ECN [21].

The discretization of time is set after the Courant number [23]. The time step is selected for the minimum number of PISO correctors to ensure computation stability and convergence. In order to optimize the computation in terms of "accuracy-stability" we used Monotone Advection Reconstruction Scheme (MARS) with blending factor 0.5. MARS is a multidimensional second-order accurate differencing scheme. It possesses the least sensitivity of solution accuracy to the mesh structure and skewness. The complete duration of spray combustion was considered to match that of the experiment. The fuel was injected with spray characteristics adjusted according to the spray characteristics applied in the experiments. In the spray model, atomization proceeded according to the Reitz-Diwakar model, and the fuel droplets were formed according to the Reitz-Diwakar breakup model [24-27]. After a reliable grid size was identified, the lift-off length was evaluated. The ECFM3Z model was used to simulate the lift-off length with the conditions in the constant volume combustion chamber, as shown in Tables 1 and 2, available from ECN [21].

Table 1. Simulation condition

Fuel @Temp	n-Heptane@373 K
Nozzle	$D_{orifice}$=0.100 mm, C_D=0.86, L/D-4.0, θ/2=6.5°
Injection pressure, ΔP	150 MPa
Ambient gas density	14.8 kg/m^3, 30.0 kg/m^3
Ambient gas temperature	1000 K

Table 2. Ambient gas composition

Molecular percentage					
O_2	N_2	CO_2	H_2O	MW	(A/F)st
21.00	69.33	6.11	3.56	29.47	15.40
15.00	75.15	6.22	3.63	29.25	21.40
12.00	78.07	6.28	3.65	29.13	26.70
10.00	80.00	6.33	3.67	29.05	32.00

The autoignition in the present simulations was controlled by the double-delay autoignition model for ECFM3Z. The double-delay autoignition model considers the effect of cool flames, which is characterized by a weak increase in temperature after the initial delay, followed by a slow-down of the reaction rates until the second delay. After this second delay, the reaction rate increases rapidly, and the main autoignition takes over. This model makes use of pre-computed tables containing the results of complex chemistry calculations of the autoignition of n-Heptane with 800 reactions and 100 species [23, 28]. The tables give values for the two delays, which are functions of pressure, temperature, equivalence ratio and the EGR rate.

The mean scalar dissipation rate χ_{st} was extracted along the mean stoichiometric mixing line. To determine the scalar dissipation rate along the stoichiometric line of mixture fraction, the iso-surface of mixture fraction values at a specific stoichiometry is created, as shown in Figure 2.

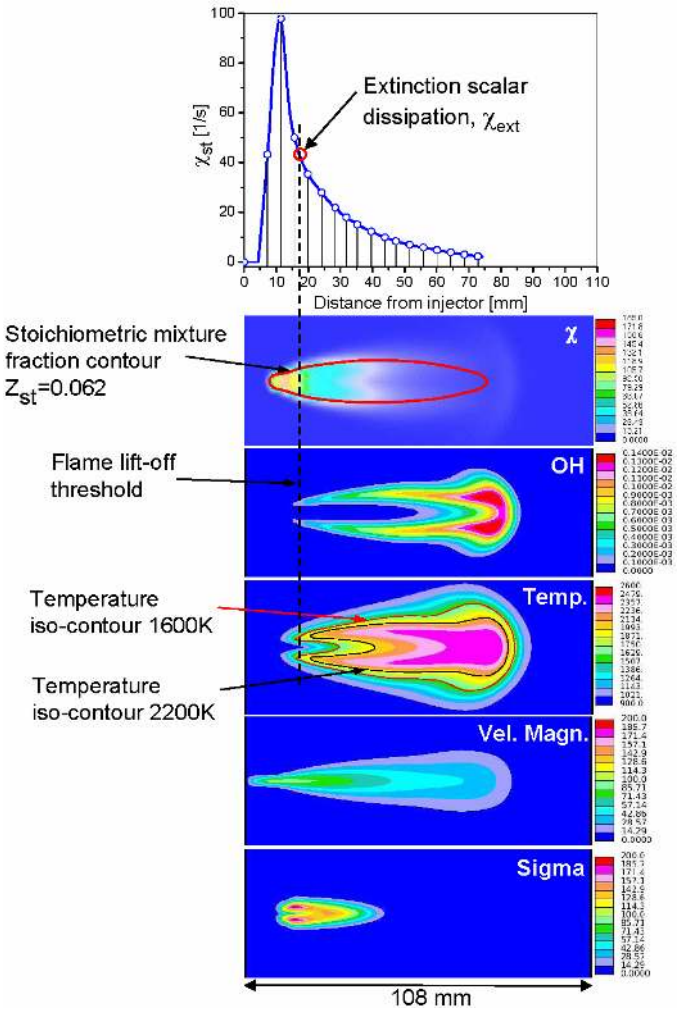

Figure 2. Assessment of the flame lift-off length. Top figure: extinction scalar dissipation value on the stoichiometric scalar dissipation curve.

The red contour in the first image of Figure 2 is a stoichiometric mixture fraction line. Computed values of the scalar dissipation rate are mapped to the iso-surface [29]. Then based on the temperature and Damkohler number relation (S-curve), the flame temperature along the stoichiometric line is plotted versus the inverse of the scalar dissipation rate. To determine the scalar dissipation rate at extinction, the threshold flame temperature of 1600K is used. This threshold flame temperature is adopted according to the conceptual model of diesel combustion presented by Dec [10] and the analysis of the overall chemical kinetics and potential sequence of reactions in hydrocarbon oxidation by Flynn *et al.* [30]. χ_{st} is plotted versus the distance along the jet penetration, and the χ_{st} value that was determined from temperature curve is projected on the graph "χ_{st} vs. distance from injector". That value on the χ_{st} graph is the value of the scalar dissipation rate at extinction, χ_{ext}, which corresponds to the flame lift-off length. Details of this procedure are explained in [29]. The computed lift-off length values were compared with experimental data from ECN of Sandia National Laboratories [21].

5. Results and discussion

5.1 Non-reacting spray

The problem of mesh dependence for the vaporizing liquid spray injected into a

constant volume chamber is illustrated in Figure 3. All computations were performed under the same conditions mentioned in section 4. The only parameter that was varied was the grid resolution. As this figure shows, grid size has an ambivalent effect on spray penetration. The use of a larger number of cells decreased the penetration of the spray. When the cell size is larger than 1mm, the penetration was longer, but when the cell size is smaller than 1mm, penetration becomes shorter with a large increase in the spray cone angle.

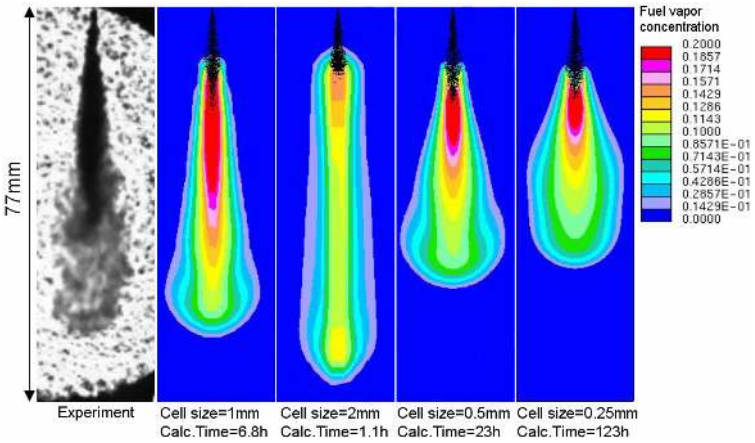

Figure 3. Comparison of vaporizing spray penetration from shadowgraph experiment with simulation at different grid resolutions. T_{amb}=820 K, P_{amb}=4 MPa, P_{inj}=135 MPa, $D_{orifice}$=0.163 mm.

As shown in Figure 4, the computed vapor penetration is slightly under-predicted. This under-predicted vapor penetration is consistent with a well known shortcoming of eddy viscosity turbulence models for free shear flow, where the models over-predict the spreading rates and consequently under-predict the penetration in round jet flows [31]. In addition, Magi *et al.* [32] found that over-prediction of the spreading rates for round gas jets persists for CFD simulations based on RANS grids and standard k-ε turbulence models.

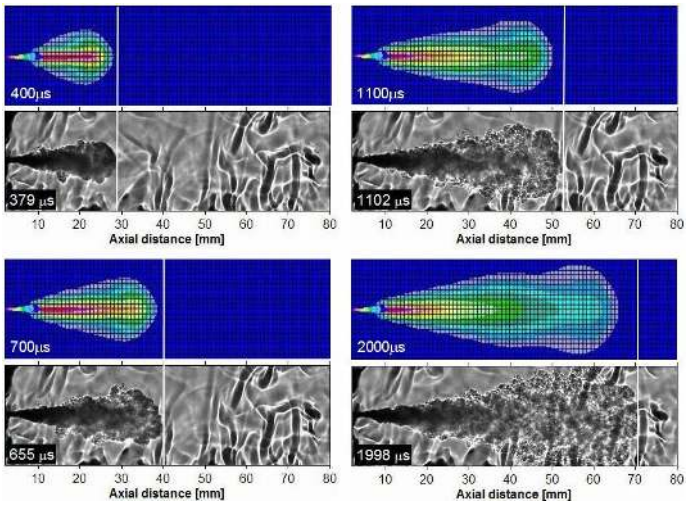

Figure 4. Penetration of n-Heptane vaporizing spray. T_{amb}=1000K, ΔP_{inj}=150MPa, $D_{orifice}$=100μm, grid size = 1mm. Experimental data of shadowgraph experiment for comparison were taken from ECN of Sandia National Laboratories [21].

Nevertheless, one possibility of reducing the effect of grid is the use of spray adapted grid such that the spray is always more or less perpendicular to the cells and is correlated with experimental results for non-vaporizing and vaporizing spray penetration, which

exactly was demonstrated here. Therefore, a computation domain with 1mm grid size was selected for further analysis on reacting spray and lift-off length.

5.2 Reacting spray

5.2.1 Flame lift-off length

The lift-off length values computed in this study using flame area density and the laminar flamelet approach showed good agreement with experimental data as well as with the numerical results obtained by other researchers. As O_2 decreases, the stoichiometric mixture fraction Z_{st} decreases, and that the stoichiometric contour is located at radial positions farther away from the centerline of the jet. Since the scalar dissipation rate, χ_{st} decreases as we move radially out from the centerline, lower O_2 leads to lower χ_{st} values in the jet. The net effect is a higher lift-off length. The assessment of lift-off length based on the extinction concept is shown in Figure 2. The computed values of lift-off length in this study were compared with the closest distance from the injector orifice to the contour of flame temperature at 1600 K, and with the distance from the injector orifice to the closest location of OH concentration. The iso-temperature value of 1600K was used considering the results of analysis of the overall chemical kinetics and potential sequence of reactions in hydrocarbon oxidation [10, 30].

The results suggest that the axial location of OH concentration that is the closest to the injector orifice, matches well the region of temperature at 1600 K, closest to the injector orifice. The extinction scalar dissipation point also corresponds to the flame temperature at 1600 K. As the jet progresses downstream from the injector, the scalar dissipation rate decreases and the lift-off length stabilizes at a certain distance from the injector. A distribution of the flame surface density (Sigma) is indicated at the location of the lift-off.

Experimental results of the Sandia combustion chamber were used to validate the present approach. The experimental flame lift-off length was measured as described in [1, 33]. Time-averaged, line-of-sight images of light emitted from a burning fuel jet at 310 nm were acquired with an intensified CCD camera using a 310 nm band-pass filter (10 nm FWHM). Figure 5 shows that the lift-off length is predicted based on the comparison of OH distributions. The results of the computed lift-off length were compared with the available experimental data at ρ_{amb}=14.8 kg/m^3, O_2-21%, O_2-15%, O_2-12% and O_2-10% from ECN [21] at the conditions listed in Table 1. It is seen that lift-of lengths estimated from OH distribution were slightly underpredicted for lower O_2 concentration cases. However, it worked reasonably well for the O_2-21%.

The results also indicated that increasing the ambient gas density increases the extinction scalar dissipation rate, χ_{ext}, and therefore, decreases the lift-off length, as shown in Figure 6. The increase in χ_{ext} is attributed to enhanced reaction rates at higher gas densities. The higher values of χ_{ext} occur closer to the injector orifice. There is also an additional influence of the changes in χ_{st} in the jet as the density is increased. χ_{st} typically decreases and the lower values of χ_{st} result from greater spreading of the jet with increase in the ambient gas density. Experimental and computed lift-off length values for the range of conditions in this paper are shown in Table 3.

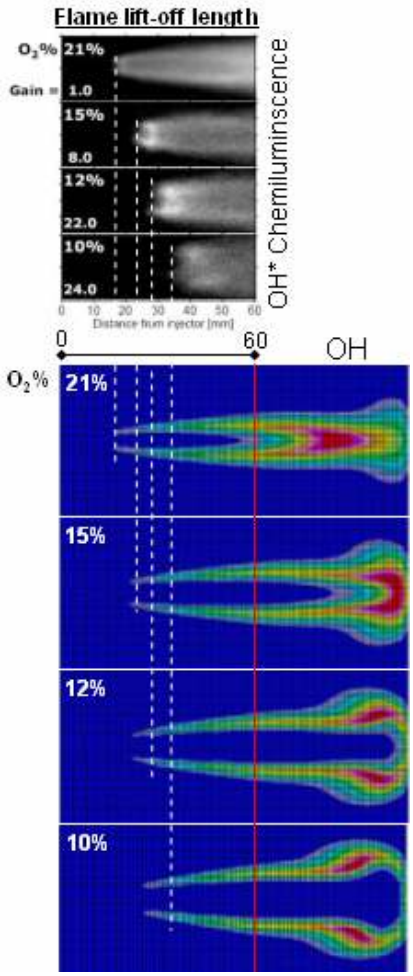

Figure 5. Comparison of experimental and computed lift-off lengths at different ambient gas oxygen concentrations. Dash lines indicate locations of lift-off lengths. Experimental data of OH* chemiluminescence experiment for comparison were taken from [34].

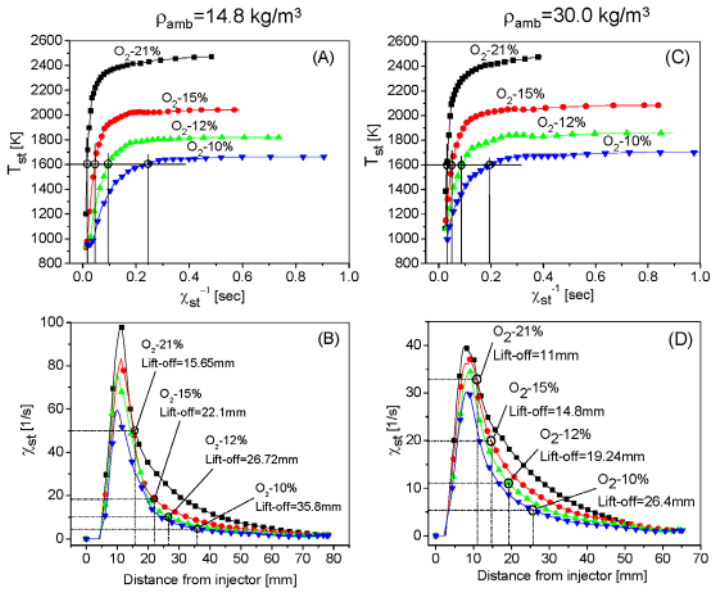

Figure 6. Temperature (A) and (C) and scalar dissipation rate (B) and (D) along the stoichiometric mixture fraction line, with predicted lift-off lengths at ρ_{amb}=14.8 and 30 kg/m^3. T_{amb}=1000K, ΔP_{inj}=150MPa and $D_{orifice}$=0.100mm.

Table 3. Experimental and simulated lift-off length values

	Lift-off length							
O_2	21%		15%		12%		10%	
ρ_{amb} (kg/m^3)	14.8	30.0	14.8	30.0	14.8	30.0	14.8	30.0
Experiment	17.00	-	23.40	11.90	29.20	13.90	35.10	16.40
Simulation	15.65	11.00	22.10	14.80	26.72	19.24	35.80	26.40

As shown in Figure 7, the stoichiometric mixture fraction fluctuations are the strongest at the high scalar dissipation rates. According to Peters [1], the large mixture fraction fluctuations in the mixture fraction space extend to sufficiently lean and reach mixtures such that the diffusion layers surrounding the reaction zone are separated. For small mixture fraction fluctuations, which may be due to intense mixing or to partial premixing of the fuel stream, the reaction zones are connected. As the flame jet progresses downstream from the injector, the scalar dissipation rate decreases and mixture fraction fluctuations become smaller than the reaction zone thickness and even the reaction zones become connected. At this condition, the mixture fraction field is nearly homogeneous, and the flame lift-off length stabilizes at a certain distance from the injector.

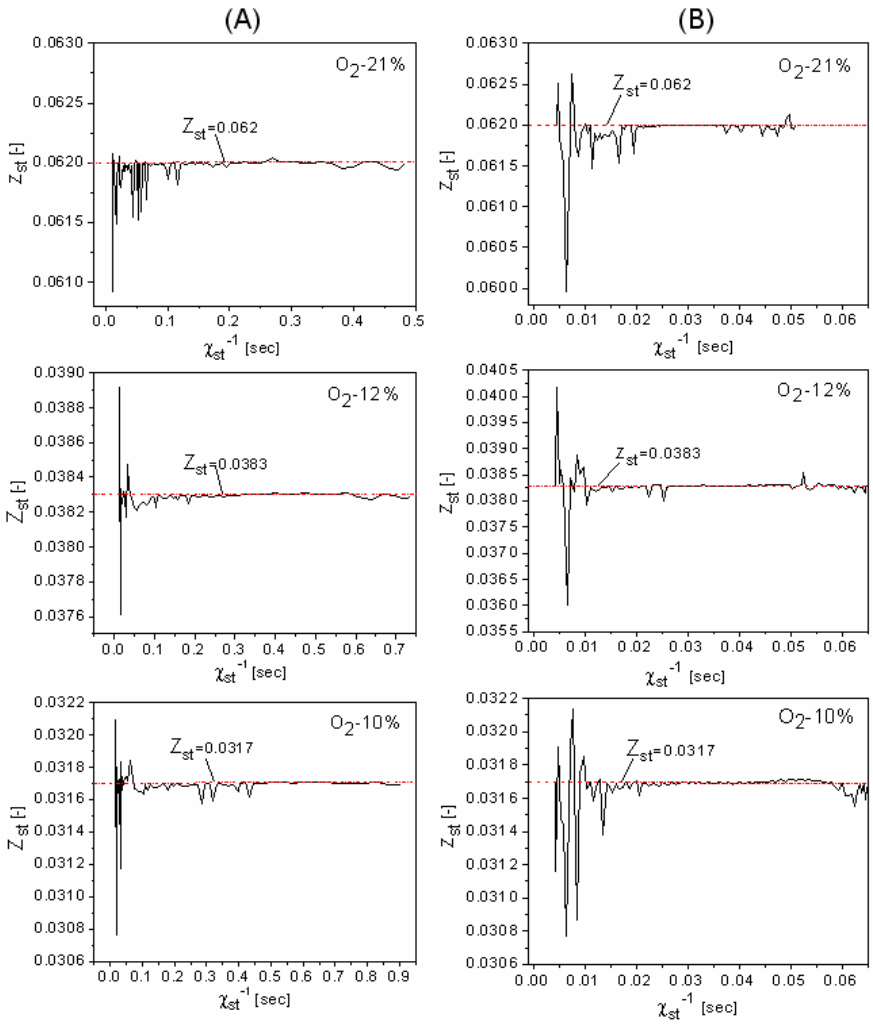

Figure 7. Stoichiometric mixture fraction fluctuation for different oxygen concentrations at (A) ρ_{amb}-14.8 kg/m^3 and (B) ρ_{amb}-30 kg/m^3

5.2.2 Heat release rate

A comparison between experimental [21] and computed pressure rates is displayed in Figure 8, for the conditions computed using double-delay autoignition model. For double-delay auto-ignition, the apparent heat release rate (AHRR) profile showed a little difference with that of experiment. Very rapid AHRR was observed before the start of the main ignition. This fast heat release is due to cool flame reactions. Pickett et al. [6] showed that exited state species are formed during the first stage of cool flame chemistry period of ignition. They identified the region where the cool flame chemistry occurs prior to high-temperature combustion.

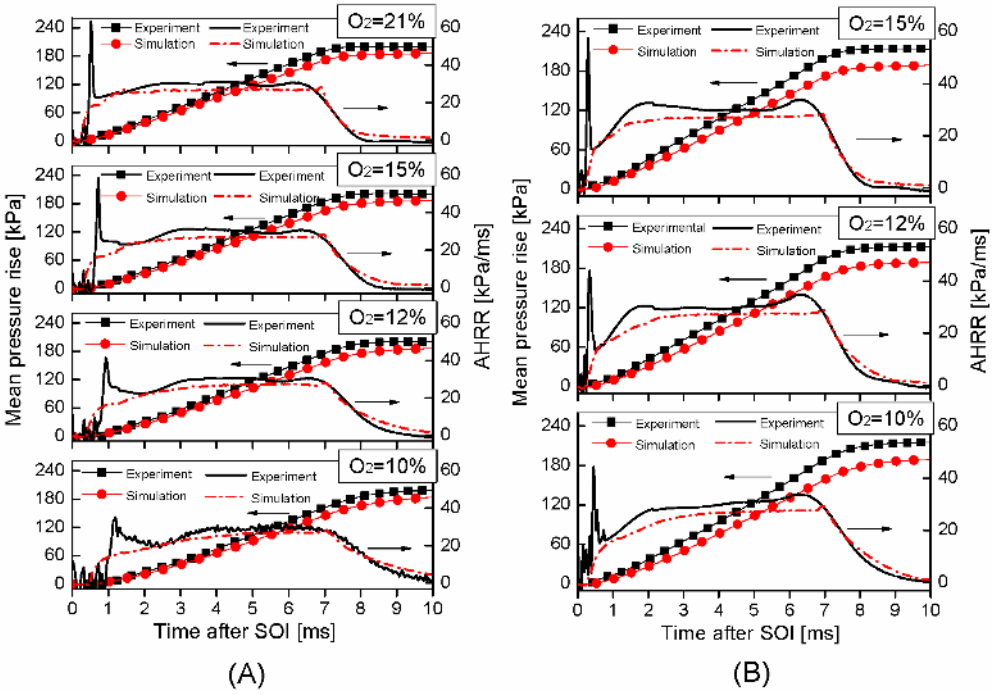

Figure 8. Pressure rise and AHRR with double-delay autoignition model at (A) ρ_{amb}-14.8 kg/m^3 and (B) ρ_{amb}-30 kg/m^3

AHRR during the premixed burn decreases with decreasing O_2 concentration. Possible reasons for this decrease include slower chemical kinetics because of dilution, or lack of oxygen entrainment because of reduced ambient oxygen. However, as the combustion proceeds, the heat release rate with reduced O_2 in mixing-controlled part of combustion becomes almost equal to the heat release rate with O_2-21%. Although the AHRR profile, in general, computed with double-delay autoignition model differs from that of the experiment, it fairly predicted the main ignition delay as it did in the experiment. The different AHRR profiles in the double-delay model may be the cause of the temporal and spatial discretizations of the computational domain, fuel evaporation model and air-fuel mixing model. The influence of these aspects will be considered in future studies. Nevertheless, the effect of cool flame on combustion should not be underestimated. In particular, for the practical implementation of the LTC concepts, using the double-delay autoignition model may be very useful for obtaining insights about the influence of ignition processes on the flame lift-off length.

In order to evaluate the cause of mixing model, the mass fraction of the fuel burned in the diffusion zone of the ECFM3Z model was computed. Figure 9 shows that as the O_2 concentration in ambient gas decreases, the mass fraction of the fuel that has been consumed by diffusion mode also decreases. The more the O_2 concentration is reduced, the

longer the ignition delay, and more the fuel is premixed with ambient gas and burned in the premixed mode, meaning that air-fuel mixing is well represented.

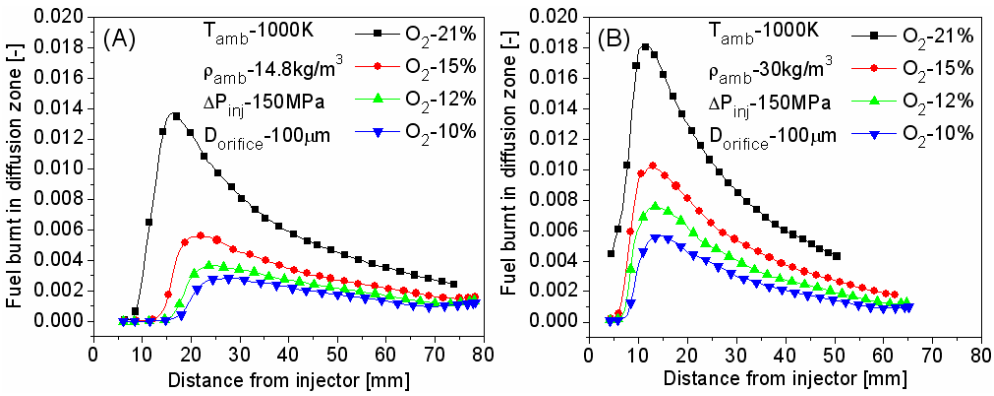

Figure 9. Mass fraction of fuel burned in diffusion zone at (A) ρ_{amb}-14.8 kg/m^3 and (B) ρ_{amb}-30 kg/m^3

6. Conclusion

A description of a novel approach to evaluate the lift-off length using the ECFM3Z model was presented. The results of this numerical study provide a comprehensive picture of the parameters affecting the diesel flame lift-off length. The computed results were compared with available experimental data from Engine Combustion Network developed by Sandia National Laboratories.

For the range of conditions investigated, adequate quantitative agreement was obtained with the experimental measurements of lift-off length under different ambient gas oxygen concentrations and ambient gas densities. The results showed that the computed values of lift-off length lay in a reasonable range within the experimental values of quasi-steady lift-off length.

The lift-off length was predicted well for the O_2-21% concentration case. However, it was slightly underpredicted for O_2-10% concentration case. These results indicate that the model is suitable for conventional diesel combustion and low EGR conditions while additional enhancements are needed for high EGR conditions.

Double-delay ignition model could not predict well the premixed phase of the AHRR profile, based on comparison of its predictions with the result of the experiment. This may be the cause of the spatial discretization of the computational domain, fuel evaporation model and air-fuel mixing model.

Acknowledgements

The authors are grateful to the Japan Society for the Promotion of Science (JSPS) for providing partial funding for this work.

References

[1] Peters, N. Turbulent Combustion. (2000). Cambridge University Press, New-York.
[2] Kalghatgi, G.T. (1984). Lift-off heights and visible flame length of vertical turbulent jet diffusion flames in still air. Combust. Flame 41, pp.17-19.
[3] Pitts, W.M. (1989). Importance of isothermal mixing processes to the understanding of lift-off and blowout of turbulent jet diffusion flames. Combust. Flame 76, pp.197-312.

[4] Schefer, R.W., Namazian, M., Kelly, J. (1994). Stabilization of lifted turbulent-jet flames. Combustion and Flame 99, pp.75-86.
[5] Tackle, M.M., Geyer, D., Hassel, E.P., Janicka, J. A detailed investigation of the stabilization point of lifted turbulent diffusion flames. Twenty-Seventh Symposium (International) on Combustion, The Combustion Institute, Pittsburgh, pp.1157-1165.
[6] Pickett, L.M., Siebers, D.L., Idicheria, C.A. (2005). Relationship between ignition processes and the lift-off length of diesel fuel jets. SAE Paper No. 2005-01-3843.
[7] Siebers, D. and Higgins, B. (2001). Flame lift-off on direct-injection diesel sprays under quiescent conditions. SAE Paper No. 2001-01-0530.
[8] Pickett, L.M., Siebers, D.L. (2004). Soot in diesel fuel jets: Effects of ambient temperature, ambient density, and injection pressure. Combust. Flame 138, p.114.
[9] Chomiak, J., Karlsson, A. (1996). Flame lift-off in diesel sprays. Proc. Combust. Inst. 26, pp.2557.
[10] Dec, J.E. (1997). A conceptual model of DI diesel combustion based on laser-sheet imaging. SAE Paper No. 970873.
[11] Senecal, P.K., Pomraning, E., Richards, K.J., Briggs, T.E., Choi, C.Y., McDavid, R.M., Patterson, M.A. (2003). Multi-dimensional modeling of direct-injection diesel spray liquid length and flame lift-off length using CFD and parallel detailed chemistry. SAE Paper No. 2003-01-1043.
[12] Tap, F.A., Veynante, D. (2005). Simulation of flame lift-off on a diesel jet using a generalized flame surface density modeling approach. Proc.Combustion Institute 30, pp.919-926.
[13] Lehtiniemi, H., Mauss, F., Balthasar, M., Magnusson, I. (2006). Modeling diesel spray ignition using detailed chemistry with a progress variable approach. Combust. Sci. and Tech. 178, pp.1977-1997.
[14] Venugopal, R., Abraham, J. (2007). A numerical investigation of flame lift-off in diesel jets. Combust. Sci. and Tech. 179, pp.2599-2618.
[15] Venugopal R. and Abraham, J. (2007). A review of fundamental studies relevant to flame lift-off in diesel jets. SAE Paper No. 2007-01-0134.
[16] D'Errico, G., Ettorre, D., Lucchini, T. (2007). Comparison of combustion and pollutant emission models for DI diesel engines. SAE Paper No. 2007-24-0045.
[17] Singh, S., Reitz, R.D., Wickman, D., Stanton, D., Tan, Zh. (2007). Development of a hybrid, auto-ignition/flame-propagation model and validation against engine experiments and flame lift-off. SAE Paper No. 2007-01-0171.
[18] Campbell, J.W., Gosman, A.D., Hardy, G. (2008). Analysis of premix flame and lift-off in diesel spray combustion using multi-dimensional CFD. SAE Paper No. 2008-01-0968.
[19] Vishwanathan, G., Reitz, R.D. (2008). Numerical predictions of diesel flame lift-off length and soot distributions under low-temperature combustion conditions. SAE paper No. 2008-01-1331.
[20] Karrholm, F. P., Tao, F., Nordin, N. (2008). Three-dimensional simulation of diesel spray ignition and flame lift-off using OpenFOAM and KIVA-3V CFD codes. SAE Paper No. 2008-01-0961.
[21] Engine Combustion Network. Sandia National Laboratories, USA. Available at http://www.ca.sandia.gov/ECN.
[22] Colin, O. and Benkenida, A. (2004). The 3-zones Extended Coherent Flame Model (ECFM3Z) for computing premixed/diffusion combustion. Oil &Gas Sci. Technology 59, 6, 593-609.
[23] STAR-CD Methodology, v3.26. pp.11-3, 10-28.
[24] Reitz, R.D. and Bracco, F.B. (1979). On the dependence of spray angle and other spray parameters on nozzle design and operating conditions. SAE Paper No. 790494.

[25] Reitz, R.D. (1987). Modeling atomization processes in high pressure vaporizing sprays. Atomization and Spray Technology 3, p.309

[26] Reitz, R.D. and Diwakar, R. (1987). Structure of high-pressure fuel spray. SAE Paper No. 870598.

[27] Reitz, R.D., 1988. Modelling atomization processes in high pressure vaporizing sprays. GMRL Publication, GMR-6017, Detroit, MI.

[28] Subramanian, G. (2007). Modeling engine turbulent auto-ignition using tabulated detailed chemistry. SAE Paper No. 2007-01-0150.

[29] Azimov, U.B. (2009). Experimental and numerical studies of diesel low-temperature combustion under quiescent conditions. PhD Dissertation, Chonnam National University, South Korea.

[30] Flynn, P. F., Durrett, R. P., Hunter, G. L., Zur Loye, A. O., Akinyemi, O. C., Dec, J. E. and Westbrook, C. K. (1999). Diesel combustion: An integrated view combining laser diagnostics, chemical kinetics, and empirical validation. SAE Paper No. 1999-01-0509.

[31] Wilcox, D.C. (1998). Turbulence Modeling for CFD. DCW Industries, 1998.

[32] Magi, V., Iyer, V., Abraham, J. (2001). The k-epsilon model and computed spreading rates in round and plane jets. Numerical Heat Transfer, Part A, 40, pp.317-334.

[33] Siebers, D.L., Higgins, B.S. (2001). Measurement of the flame lift-off location on DI diesel sprays using OH chemiluminescence. SAE Paper No. 2001-01-0918.

[34] Idicheria, C.A., Pickett, L.M. (2005). Soot formation in diesel combustion under high-EGR conditions. SAE Paper 2005-01-3834.